Title: Trapping the enemy: *Vermamoeba vermiformis* circumvents Faustovirus mariensis dissemination by enclosing viral progeny inside cysts

Running title: *Vermamoeba vermiformis* traps faustovirus inside cysts

Authors: Iara Borges[1], Rodrigo Araújo Lima Rodrigues[1], Fábio Pio Dornas[2], Gabriel Almeida[3], Isabella Aquino[1], Cláudio Antônio Bonjardim[1], Erna Geessien Kroon[1], Bernard La Scola[4], Jônatas Santos Abrahão[1*]

Affiliations

1 Laboratório de Vírus, Instituto de Ciências Biológicas, Departamento de Microbiologia, Universidade Federal de Minas Gerais, Belo Horizonte, MG, 31270-901, Brazil.

2 Universidade Federal dos Vales do Jequitinhonha e Mucuri, Diamantina, Brazil

3 Department of Biological and Environmental Science, University of Jyvaskyla, FI-40014 Jyvaskyla, Finland.

4 URMITE, Aix Marseille Université, UM63, CNRS 7278, IRD 198, INSERM 1095, IHU - Méditerranée Infection, 19-21 boulevard Jean Moulin, 13005 Marseille, France

* Corresponding author: jonatas.abrahao@gmail.com

Keywords: faustovirus; vermoameba; cysts; antiviral; virus control

Abstract

Viruses depend on cells to replicate and can cause considerable damage to their hosts. However, hosts have developed a plethora of antiviral mechanisms to counter-attack or prevent viral replication and to maintain homeostasis. Advantageous features are constantly being selected, affecting host-virus interactions, and constituting a harsh race for supremacy in nature. Here we describe a new antiviral mechanism unveiled by the interaction between a giant virus and its amoebal host. Faustovirus mariensis infects *Vermamoeba vermiformis*, a free-living

amoeba, and induces cell lysis to disseminate into the environment. Once infected, the cells release a soluble factor that triggers the encystment of neighbor cells, preventing their infection. Remarkably, infected cells stimulated by the factor encyst and trap the viruses and viral factories inside cyst walls, which are no longer viable and cannot excyst. This unprecedented mechanism illustrates that a plethora of antiviral strategies remains to be discovered in nature.

Importance

Understanding how viruses of microbes interact with its hosts is not only important from a basic scientific point of view, but also for a better comprehension of the evolution of life. Studies involving large and giant viruses have revealed original and outstanding mechanisms concerning virus-host relationships. Here we report a mechanism developed by *Vermamoeba vermiformis*, a free-living amoeba, to reduce Faustovirus mariensis dissemination. Once infected, *V. vermiformis* cells release a factor that induces the encystment of neighbor cells, preventing infection of further cells and/or trapping the viruses and viral factories inside the cyst walls. This phenomenon reinforces the need for more studies regarding large/giant viruses and their hosts.

Introduction

Virion release and dissemination are *sine qua non* conditions for the maintenance of most of viral species in nature. Evolutionary constraints have shaped a variety of mechanisms promoting viral particle release and dissemination from infected cells; these range from mature virions budding through the cell membrane to virus-induced cell lysis. As a response, hosts have developed mechanisms to block or reduce viral particle propagation, replication, or both through host-populations in a constant struggle against viruses. The Red Queen theory illustrates such a race for supremacy, in which advantageous features are selected, and these changes, at least

temporarily and spatially, the balance of the interaction to one of the sides. Examples of hosts limiting viruses can be found in many groups of organisms, from bacterial anti-bacteriophage defenses (1), to plants silencing viral genes (2), and to the importance of pattern recognition receptors (PRRs), capable of triggering immune responses for multicellular host species (3). As remarkable example, the interferon (IFN) system acts as a major player against viral propagation in vertebrates (4–6). Host cells recognize viral molecules through PRRs, resulting in signaling pathways that lead to the production of IFN molecules. These are secreted and act in paracrine and autocrine ways by activating a second round of signaling, this time responsible for establishing an antiviral state, which leads to cell death in the case of infection. Although some cells are infected and lysed, IFN signaling reduces virus propagation and total viral load (6).

In this context, comprehensive studies involving large and giant viruses have revealed original and outstanding mechanisms concerning virus-host relationships. A complex interaction involving three players has been described for the free-living protist *Cafeteria roenbergensis*, in which a provirophage (mavirus), integrated in the genome of the protist, imparts a partial protection to *C. roenbergensis* populations in case of an eventual infection by a lytic giant virus called Cafeteria roenbergesis virus (CroV) (7). It has been also demonstrated that haploid cells (but not diploid cells) of *Emiliania huxleyi*, a free-living marine protist, are refractory to Emiliania huxleyi virus 86 infection in an evasion mechanism known as Cheshire Cat (8). Analogously, our team described the same phenomenon for free-living amoebas belonging to the *Acanthamoeba* genus, in which the cysts, but not the trophozoitic forms, are resistant to mimivirus infection (9, 10). We have demonstrated that once infected by mimivirus, *Acanthamoeba* trophozoites are no longer able to encyst, because mimivirus blocks the expression of a serine proteinase gene, a canonical element involved in the encystment process(10). Although it has been described that *Acanthamoeba* trophozoites are able to encyst in the presence of some intracellular bacteria (11), this phenomenon has never been described during amoebal virus infections.

Here we report a mechanism developed by *Vermamoeba vermiformis*, a free-living amoeba, to reduce Faustovirus mariensis dissemination and consequently protect neighbor cells. Once infected, *V. vermiformis* cells release a non-proteic soluble factor that induces the encystment of neighbor cells, preventing infection of further cells, since Faustovirus is only able to infect trophozoites. Interestingly, if cells already infected are exposed to the soluble encystment factor, they encyst and trap the viruses and viral factories inside the cyst walls. Unlike what has been described for amoebal cysts containing intracellular bacteria, cysts enclosing Faustovirus particles, factories, or both are no longer viable and cannot excyst, thus trapping viral progeny irreversibly inside the thick cyst walls and promoting an effective reduction of viral load on, and dissemination to, the amoebal population.

Results

1. Faustovirus mariensis: isolation and genomic analysis

Attempting to isolate new amoebal viruses, we performed collections of surface water samples at Pampulha Lagoon in Belo Horizonte, Brazil. One of the samples, collected in front of Pampulha Art Museum (Figure 1A), induced a cytopathic effect (CPE) in *V. vermiformis*, a free-living amoeba occurring worldwide, and already described as one of the hosts of some giant or large viruses, including Faustovirus, Tupanvirus, Kaumoebavirus, and Orpheovirus. Cells presenting CPE were submitted to transmission and scanning electron-microscopy (TEM and SEM), revealing viral particles similar to Faustoviruses, with approximately 190 nm, icosahedral symmetry and a capsid containing an electrodense central region (genome) (Figures 1B–1D). We named this new isolate Faustovirus mariensis. During virus propagation and purification, we observed that F. mariensis induces the formation of plaque forming units, a CPE never described for any other amoebal giant virus, according to our knowledge (Figures 1E–1F). During the time-course of infection, plaque units expand and coalesce in *V. vermiformis* monolayers (Figure 1G).

The genome of F. mariensis is a circular double-stranded DNA molecule of 466,080-bp length (See Fig. S1 at https://5c95043044c49.site123.me/my-blog/supp-material-trapping-the-enemy-vermamoeba-vermiformis-circumvents-faustovirus-mariensis-dissemination-by-enclosing-viral-progeny-inside-cysts). The GC content is 36%, and it was predicted to encode 483 genes (210 located at negative strand; 273 at positive strand), with a coding density of 90%. The predicted proteins had a mean length (± standard deviation) of 279 ± 258 amino acids (ranging from 53 to 2980 amino acids). A total of 374 proteins (77.4%) had no known function (Figure 2A). The major functional gene categories were represented by DNA replication, recombination and repair, as well as transcription and RNA processing, with 22 and 25 genes, respectively (Figure 2A), with additional genes for DNA polymerase, D5 primase helicase, topoisomerase II, different subunits of DNA-directed RNA polymerase, mRNA capping enzymes, transcription factors, among others. No tRNA was predicted and no ORFans were detected. Differently from other giant viruses, only one translation factor is encoded by F. mariensis, the translation initiation factor SUI1, which was the only translation-related gene also observed in Faustovirus E12, the first member of this new group of viruses to be described (12). Other genes previously described for faustoviruses were also encoded in F. mariensis. These include two adjacent polyproteins of 220 kDa and 60 kDa, a ribosomal protein acetyltransferase, and some genes belonging to large paralogous families, such as membrane occupation and recognition nexus (MORN) repeat-containing proteins, and ankyrin repeat-containing proteins, although only two genes were found to have this repeat domain (Figure 2A). Synteny analysis revealed a highly conserved genome organization among faustoviruses. However, the F. mariensis genome exhibited a small region (~11.5 kb) that was rearranged in its genome in regards to the other described faustoviruses, i.e., the region was located after a conserved block of >30 kb in F. mariensis and before that block in other viruses (See Fig. S2 at https://5c95043044c49.site123.me/my-blog/supp-material-trapping-the-enemy-vermamoeba-vermiformis-circumvents-faustovirus-mariensis-dissemination-by-enclosing-viral-progeny-inside-cysts). This region comprised 18 genes, most of them with unknown functions. The analysis of DNA polymerase, a marker used for phylogenetic analysis of nucleocytoplasmic

large-DNA viruses (NCLDVs) confirmed that F. mariensis was clustered with other Faustovirus isolates, and was more related to the clade containing Faustovirus E12 (Figure 2B).

2. Faustovirus mariensis replication cycle

The analyses of the F. mariensis replication cycle in *V. vermiformis* were performed based on asynchronical infection (multiplicity of infection (MOI) of 0.1), starting from fresh trophozoites, and purified viral particles. We analyzed whether *V. vermiformis* cysts would be permissive to F. mariensis infection, but neither cytopathic effects nor increases in viral loads were observed; therefore, Faustovirus, as has been described for mimivirus, needs to infect amoebal trophozoites to start its replication cycle. In the cytoplasm of trophozoites, F. mariensis induced the formation of large electron-lucent viral factories (about 3.5 µm length) frequently observed close to the cell nucleus (Figures 3A–3C). Viral infection induced the recruitment of mitochondria to the periphery of viral factory, suggesting virus-induced energy optimization during viral morphogenesis (Figures 3A and 3C). Curiously, intranuclear particles were also observed but further studies are necessary to determine their role in the F. mariensis replication cycle (See Fig. S3 at https://5c95043044c49.site123.me/my-blog/supp-material-trapping-the-enemy-vermamoeba-vermiformis-circumvents-faustovirus-mariensis-dissemination-by-enclosing-viral-progeny-inside-cysts).

As observed for other viruses of free-living amoebae (13–16), F. mariensis morphogenesis began with crescents, open structures of approximately 50 nm, which grew as the electron-dense material of the viral factory fulfilled them (Figure 4A). Particles of almost 200 nm without genomic content were observed in the late phases of morphogenesis, when the genome was incorporated and centralized within several newly formed viral particles (Figure 4A). Faustovirus mariensis progeny were organized in a honeycomb fashion inside viral factories, as previously described for other Faustovirus isolates (12) (Figure 4B-E). Small honeycombs expanded as new mature viruses formed and coalesced to others in the cytoplasm (Figure 4B). By the end of the replication cycle, the cytoplasm was fully taken by new F. mariensis particles (See Fig. S4 at https://5c95043044c49.site123.me/my-blog/supp-material-

trapping-the-enemy-vermamoeba-vermiformis-circumvents-faustovirus-mariensis-dissemination-by-enclosing-viral-progeny-inside-cysts). Contrary to what has been described for Marseillevirus and Pandoravirus, exocytosis was not observed (16). Cellular lysis is likely the most important form of liberation of newly formed F. mariensis particles. Isolated particles or aggregates of F. mariensis associated with cellular structures were observed extracellularly, and aggregates became as large as a trophozoite of *V. vermiformis* (See Fig. S4 at https://5c95043044c49.site123.me/my-blog/supp-material-trapping-the-enemy-vermamoeba-vermiformis-circumvents-faustovirus-mariensis-dissemination-by-enclosing-viral-progeny-inside-cysts).

3. *V. vermiformis* cells may encyst and trap F. mariensis particles and factories inside cyst wall

Interestingly, during routine production and titration of F. mariensis, we observed a substantial formation and accumulation of *V. vermiformis* cysts, especially when cells were infected at high MOIs (1 and 10). This curious effect drew our attention, and we decided to verify whether other viruses would be able to trigger encystment. However, *V. vermiformis* infection with Tupanvirus or Orpheovirus did not induce the formation and accumulation of cysts in the culture flasks, regardless the MOI (data not shown). As such phenomena seemed to be a singular characteristic of F. mariensis, we decided to further characterize it.

Hence, *V. vermiformis* cells were infected with F. mariensis at a MOI of 10 and prepared for transmission electron microscopy (TEM) (24 hpi). Remarkably, TEM images revealed F. mariensis particles and viral factories not only inside a few *V. vermiformis* trophozoites, but also within the cytoplasm of many cysts and cells under encystment (Figure 5). This phenomenon, previously described for some bacteria (*Salmonella enterica, Listeria monocytogenes, Yersinia enterocolitica, and Escherichia coli*) (11), had never been described for viruses to our knowledge. The observation of more than one hundred cysts revealed the presence of F. mariensis under distinct phases of the replication cycle, including the early viral factory formation, late morphogenesis, honeycomb formation/coalescence and, at last,

cytoplasm fulfilled by mature viral particles (Figure 6 A-F). In case of cells fulfilled by viral particles (late cycle), some cellular structures seemed to be degraded, including mitochondria and plasma membrane (Figure 6F). Despite the observation of variations in wall thickness among infected cysts, the cyst walls appeared intact and with no damage (Figure 6).

We then quantified the number of cysts of *V. vermiformis* formed after the inoculation of F. mariensis at different MOIs. A total of 3 x 10^6 trophozoites were added to T25 flasks with 5 ml of Peptone Yeast Extract Glucose (PYG) medium (this medium favors the propagation of amoebas) and inoculated at MOIs of 0.01, 0.1, 1, or 10. After adsorption, cells were washed and then incubated for 48 h with PYG medium. Uninfected cells were used as controls, and after 48 h of incubation, we measured the propagation of those cells, which reached approximately 7.8 x 10^6 cells; among those cells, we observed a natural encystment rate of approximately 21%, which is related to the reduction of nutrients in the PYG medium during the time of incubation (Figure 7A). However, *V. vermiformis* trophozoites infected by F. mariensis presented a higher rate of cysts 48 hpi, and this number was positively related to the MOI. Flasks inoculated at MOIs of 0.01 or 0.1 resulted in 63.6% and 75% of cysts, respectively; while flasks inoculated at higher MOIs, 1 or 10, both presented 100% cysts at 48 hpi (Figure 7A). Interestingly, infections with high MOIs (1 and 10) presented an encystment ratio (number of cysts obtained divided by the number of trophozoites imputed) of approximately 1:1, close to the initial input of trophozoites. These results indicated that trophozoites infected at high MOIs (1 or 10) with F. mariensis were almost totally converted to cysts (Figure 7A). We also analyzed whether F. mariensis inactivated particles (same MOI as above described) would be able to trigger *V. vermiformis* encystment, but we could not observe differences in the number of cysts between inoculated and non-inoculated cells, indicating that the triggering of encystment is dependent on virus entry and replication.

The next step was to measure F. mariensis replication in *V. vermiformis* inoculated at different MOIs. Therefore, *V. vermiformis* cells were infected with F. mariensis at MOIs of 0.01, 0.1, 1, and 10, and incubated for one week. At this stage, trophozoites were no longer observed, regardless the MOI, since they either were lysed (releasing viruses to supernatant) or

converted to cysts. This longer time of incubation was designed to allow the lysis or encystment of all trophozoites in the system; therefore, at the end of the experiments, we would find viruses only in the supernatants (originated from lysis of infected trophozoites) or inside cysts. The supernatants and cysts were separated by centrifugation and viral genome load was quantified by qPCR. A substantial replication of the virus was correlated with low MOIs, with larger amounts of DNA detected in the supernatant at MOIs of 0.01 and 0.1 (Figure 7B). Higher MOIs (1 and 10) however, presented relatively low amounts of viral DNA in the supernatant but a substantial amount inside cysts, indicating that the virus was able to initiate the infection but not to release its progeny, after having its genome (and particles) imprisoned within the newly formed cysts (Figure 7B).

4. Faustovirus infected cysts fail excystment

Studies demonstrated that several intracellular bacteria are able to survive and take advantage of amoebal encystment (11, 17). It has been suggested this feature would guarantee bacteria to be protected during adverse environmental conditions while inside the cyst. Once good environmental conditions are available, these bacteria could return to multiply and maintain their life cycle upon excystment. At a first glance, F. mariensis could possibly use this same stratagem to eventually return to replicate in new trophozoites.

To test this hypothesis, trophozoites of *V. vermiformis* were infected with different MOIs of F. mariensis diluted ten-fold from 0.01 to 10. Cysts produced after the infection were collected, washed to remove external viral particles, and then their potential of excystment was evaluated. Two different methods to trigger excystment were used: exposure of cysts to PYG media with 5% of fetal bovine serum (FBS) in T25 cell flasks, and plating of cysts on petri dishes with Bacto® Agar covered with a monolayer of heat-inactivated *Escherichia coli*.

Surprisingly, cysts derived from the higher MOIs (1 and 10) did not excyst upon either method employed (Figure 8A). Those cysts were then analyzed by TEM, revealing viral particles inside almost all of the cysts. Curiously, some of those cysts, in spite of appearing to have a typical thick wall, had a reduced diameter (about 3.5 μm) and had lost their rounded

shape (Figures 8C–8E). For cysts derived from infections with MOIs of 0.01 and 0.1, excystment was observed for nearly 24% of cells. The TEM analysis revealed that only cysts not presenting viral particles, factories, or both in their cytoplasm were able to excyst (Figure 8C). This data was confirmed by subculturing individual trophozoites obtained after excystment (from cultures inoculated at MOIs of 0.01 and 0.1), which did not show any cytopathic effect or detection of viral particles. As described for cells infected at MOIs of 1 and 10, we also observed infected cysts with reduced diameters and irregular shapes in flasks inoculated at MOIs of 0.01 and 0.1 (Figures 8C–8E).

When the viability of cysts was assayed with 0.4% trypan blue, it was revealed that 100% of cysts from cells inoculated at MOIs of 1 and 10 were no longer viable, while 46% and 57% of cysts from flasks inoculated at MOIs of 0.01 and 0.1 were not viable, respectively (Figure 8B). Although not viable, infected cysts were as resistant as uninfected cysts against hydrochloric acid and heating treatments followed by 3 cycles of sonication. They kept their walls visually intact, and preserved intracellular structures, including viruses and factories (See Fig. S5 at https://5c95043044c49.site123.me/my-blog/supp-material-trapping-the-enemy-vermamoeba-vermiformis-circumvents-faustovirus-mariensis-dissemination-by-enclosing-viral-progeny-inside-cysts). Taken together, these results indicate that *V. vermiformis* encystment was triggered by F. mariensis infection, in a MOI-dependent way. Once encysted, infected cells were no longer able to excyst, thus irreversibly imprisoning the viral progeny within their thick walls.

5. Faustovirus mariensis is unable to circumvent *V. vermiformis* encystment

Our team has previously shown that mimivirus was capable of inhibiting the process of encystment in *Acanthamoeba castellanii* by down-regulating the expression of a cellular serine protease gene, which is an essential enzyme responsible for triggering the encystment pathway in these cells (10). Once infected by mimivirus, a given trophozoite of *A. castellanii* inevitably suffers from lysis due to viral replication, since the virus blocks encystment. In contrast, when

A. castellanii trophozoites were incubated with an encystment stimulation factor (e.g. NEFF solution) previous to Mimivirus inoculation, serine proteinase gene expression was stimulated, which triggered encystment and circumvented Mimivirus replication. Therefore, avoiding or blocking the triggering of encystment is critical for amoebal virus replication, since they are able to replicate only in non-encysting trophozoites. Herein, we investigated whether F. mariensis could be able to block *V. vermiformis* encystment.

Briefly, *V. vermiformis* trophozoites were treated with NEFF solution, and 2 h later this solution was removed; the purified virus was inoculated at a MOI of 10, then flasks were added with PYG medium and incubated for 24 h. Virus genome replication was assayed by qPCR, and cells were analyzed by TEM and optical microscopy. Cell viability was analyzed using trypan blue. After 24 h, virus genome replication was not observed, and all trophozoites were converted into viable uninfected cysts (Figures 9A–9D and see Fig. S6 at https://5c95043044c49.site123.me/my-blog/supp-material-trapping-the-enemy-vermamoeba-vermiformis-circumvents-faustovirus-mariensis-dissemination-by-enclosing-viral-progeny-inside-cysts). Alternatively, we inoculated *V. vermiformis* trophozoites with F. mariensis at a MOI of 10; then, after 2 h, we treated the cells with NEFF solution, and then cells were incubated for 24 h. In this case, we detected viral genome replication inside cysts (about 6 logs, arbitrary units); and most of cysts (non-viable) had viral particles or factories in the cytoplasm (Figures 9A–9D and Fig. S6 at weblink informed above). As an experimental control, we submitted Tupanvirus, a Mimivirus relative, to the same experiments (MOI of 10). It was not possible to detect Tupanvirus genome replication in *V. vermiformis* pre-treated with NEFF; there were neither viral particles nor genomes inside cysts (Figures 9A–9D and Fig. S6 at weblink informed above). On the other hand, when *V. vermiformis* trophozoites were infected with Tupanvirus and then treated with NEFF, the virus genome was able to replicate (about four logs, arbitrary units), cells were lysed, and no cyst formation was observed (Figures 9A–9D and Fig. S6 at weblink informed above).

As previously mentioned, the encystment process is triggered after the expression of cellular serine proteinases. Such proteases' catalytic site is composed by a triad, consisting of

three amino acids: His 57, Ser 195 and Asp 102. The importance of such enzymes on *Acanthamoeba* encystment has been demonstrated by measuring the levels of serine-proteinase transcripts and protein during encystment process (9, 10). Inhibition of serine-proteinase genes transcription negatively affect encystment. We measured (by qPCR) the expression levels of two serine proteinase mRNA isotypes present in *V. vermiformis* upon infection (MOI of 10) with F. mariensis, Tupanvirus, or NEFF treatment. Five hours post-infection, F. mariensis induced significant expression of both analyzed serine proteinase isotypes ($p<0.001$), in levels comparable to those detected in cells treated with the encystment stimulation solution NEFF (Figure 9E). In contrast, Tupanvirus circumvented the expression of *V. vermiformis* serine proteinases, keeping the levels similar to uninfected or untreated trophozoites (Figure 9E). Altogether, these results suggest that F. mariensis was incapable of down-regulating factors that trigger the encystment of *V. vermiformis* as has been described for Mimivirus. Tupanvirus however, demonstrated a behavior in *V. vermiformis* similar to that of Mimivirus in *A. castellanii*.

6. Infected trophozoites release soluble factors which trigger the encystment

Previous studies have demonstrated that the secretion of soluble factors can modulate the process of encystment in *A. castellanii* (18). Although the nature of such factors remains to be better characterized, it has been suggested they could act as major players in a communication system among amoebas, stimulating cell encystment as a response to harsh conditions. To investigate whether *V. vermiformis* cells infected by F. mariensis secrete factors involved with encystment, the supernatant of a culture infected at a MOI of 10 was collected 4 dpi. The supernatant was filtered with a 0.1-µm pore size filter to remove all viral particles and subsequently diluted 2-fold to inoculate new cultures of *V. vermiformis* trophozoites.

Remarkably, we observed a strong induction of encystment in *V. vermiformis* cells in a dose-dependent fashion by the virus-free supernatant from previous F. mariensis infections. Undiluted (pure) supernatant induced the encystment of approximately 67% of cells (Figure 10A). Supernatants from *V. vermiformis* cells infected by F. mariensis at MOIs of 0.01, 0.1, and

1 were also collected, filtered, and inoculated (undiluted) to fresh *V. vermiformis* cells. Supernatants with MOIs of 0.01, 0.1, and 1 caused encystment of nearly 35%, 43%, and 65% of cells, respectively (Figure 10B). To determine the nature of this encystment factor, the supernatant was treated with different concentrations of proteinase K or bromelain (to remove proteins) and inoculated into fresh cultures of *V. vermiformis* trophozoites. The enzymatic treatment did not affect the encystment of *V. vermiformis*, suggesting that such encystment factor(s) were not proteins.

We measured the concentration of different inorganic factors in the supernatants of infected cells (MOI of 10, 10 hpi) with F. mariensis, Tupanvirus, and uninfected cells (control). Supernatants of all studied groups had similar concentrations of potassium and calcium (Figures 10C and 10D). However, we observed a significant increase in magnesium ion (Mg^{2+}) concentrations in cells infected with F. mariensis (Figure 10E). This result is consistent with previous studies that have shown Mg^{2+} as a factor able to trigger encystment in *A. castellanii* (9, 19). We then tested the potential of Mg^{2+} to induce encystment in *V. vermiformis*. First, 3 nmol of Mg^{2+} was put in a culture of 4 x 10^4 amoeba trophozoites, and the concentration of Mg^{2+} was measured, as well as the rate of cyst formation at different times. The Mg^{2+} input not only stimulated the encystment of 79% of the cells after 9 hours, but it also promoted a gradual increase of Mg^{2+} concentration during the experimental period (Figure 10F). These results suggest that once stimulated by Mg^{2+}, *V. vermiformis* trophozoites trigger an encystment program, and secrete more Mg^{2+} as an encystment stimulus for neighbor trophozoites.

Considering these results, we evaluated the effect of a bivalent cation inhibitor, ethylenediaminetetraacetic acid (EDTA), on cyst formation during F. mariensis infection, at a MOI of 10. EDTA is well known to act as an Mg^{2+} chelating agent. EDTA caused a significant reduction in cyst formation rates (Figure 10G). Our results demonstrated that EDTA promoted a significant increase in the viral genome load in the supernatants of cultures, since the viral progeny succeeded in being released from infected trophozoites, because they were not being trapped inside cysts (Figure 10H). We also observed that EDTA affected the capacity of supernatant collected from cells infected with F. mariensis to induce encystment in fresh

trophozoites in a dose-dependent way (Figure 10I), reinforcing the idea that Mg^{2+} may be one of the soluble factors released by *V. vermiformis* to stimulate encystment in neighbor cells.

Discussion

Viral sensing as well as the molecular communication within multicellular organisms or among unicellular individuals are important factors for survival in the never-ending evolutionary struggle between viruses and hosts. The ability to sense that a virus is present and respond to an infection is crucial for the host population survival. Bacterial enzymes discriminate between endogenous and foreign nucleic acids by using epigenetic cues; *Sulfolobus islandicus* (Archaea) is able to enter dormancy in response to phage presence, and quorum sensing has been shown to be important for anti-phage defense strategies in *Vibrio anguilarum* (20–22). PRRs are conserved molecules found in multicellular organisms such as plants, insects and vertebrates (23). The activation of these receptors by pathogens results in signaling pathways that lead to innate immune mechanisms aimed at controlling the infections. As the complexity of organisms increases, the immune responses become more robust. When a pathogen is sensed by PRRs in a vertebrate cell, soluble molecules (IFNs) are secreted and establish an antiviral state in any other cell that receives the IFN, besides acting on immune cells to mount an adaptive immune response (4). Although much is known about viral sensing and antiviral responses on multicellular organisms, the bases of pathogen recognition and response to infection in unicellular eukaryotes is still obscure. Understanding how viruses of microbes interact with its hosts is not only important from a basic scientific point of view, but also for a better comprehension of the evolution of life as well as discovering novel mechanisms and molecules that could be used for applied science. In recent examples, communication between viruses has been shown and described to be mediated by small peptides, while the investigation of bacterial DNA-based acquired immunity led to the recent CRISPR revolution in science and biomedicine (24–26).

Here we show that, when *V. vermiformis* faces infection by Faustovirus, it is able to trap the viruses inside cysts. The virus-containing cysts are non-viable, so the trapping process protects the uninfected amoebal population and could be considered a novel type of antiviral strategy. Our data also show that the encystment response to F. mariensis was mediated by at least one unknown encystment factor released by infected cells in conjunction with Mg^{2+}. An overview of the process is shown in Figure 10J. The putative encystment factor was not a protein, since a proteinase K/bromelain treatment did not abolish the cyst inducing ability of conditioned media. Its secretion was dependent on Faustovirus entry and replication, as conditioned media from *V. vermiformis* exposed to inactivated virions did not enhance cyst formation. Since it is unlikely that the encystment factor was derived from the virus, due to its negative impact on viral success, it is tempting to assume that viruses are being recognized by the infected amoebal cell, which in turn produces the encystment factor as a response. When this factor is secreted, nearby cells are warned of viral presence and either reversibly encyst before the infection happens or trap the viruses inside damaged cysts, thus protecting the rest of the population. This could be considered analogous to the IFN response, in which virus sensing leads to molecular communication between cells and a subsequent sacrifice of those infected in order to minimize damage to the organism population. In the case of giant viruses such as Tupanvirus and Mimivirus, escape mechanisms against the production of the encystment factor would have appeared, analogous to the myriad of evasion mechanisms possessed by viruses of vertebrates against the IFN system. Recently, Yoshikawa and co-workers demonstrated that a new remarkable giant virus called Medusavirus is able to induce encystment of *Acanthamoeba* cells as well (27). However, the mechanisms involved in such phenomenon remain to be investigated. New studies on amoebas (including *V. vermiformis*) cyst wall composition, synthesis and dynamics would be welcome to a better understanding of such processes (28). Ecological approaches would be very interesting as well, concerning how encystment factors (as Mg^{+2}) would act on lakes, rivers and oceans, and its impact on the communication of amoebas' communities, on narrow and broad scales.

The complexity of the amoebal host cell, along with the large genomes of giant viruses, makes a reductionist approach to study *V. vermiformis* and F. mariensis interactions challenging. The non-protein nature of the encystment factor(s) makes isolating it from the complex metabolomics of an amoebal cell difficult, while the large genome and elaborate particle of the virus makes pinpointing specific targets for recognition or other interactions challenging. However, our data can be considered a starting point for better comprehending ancient and unique virus-host interactions. The antiviral strategy described here is a new example of the constant race for supremacy between parasites and hosts. This unprecedented mechanism illustrates that many different antiviral strategies are yet to be unveiled in the biosphere.

Methods

Virus isolation

In August 2015, 15 water samples were collected from Pampulha Lagoon, Belo Horizonte, Brazil. The collection was performed with sterile tubes, and the samples were stored at 4 °C until the inoculation process. The samples were then subjected to filtrations through a paper filter and then through a 5 µm filter to remove large particles of sediment. For viral isolation, we used *Acanthamoeba polyphaga* (ATCC 30461), *Acanthamoeba castellanii* (ATCC 30234), and *Vermamoeba vermiformis* (ATCC CDC19). Amoebae were grown in 75 cm^2 Nunc™ Cell Culture Treated Flasks (Thermo Fisher Scientific, USA) with 30 mL of Peptone Yeast Extract Glucose (PYG) medium (29) supplemented with 0.14 mg/mL penicillin (Sigma-Aldrich, USA), 50 mg/mL gentamycin (Thermo Fisher Scientific, USA), and 2.5 mg/mL amphotericin (Bristol-Myers Squibb, New York, USA) at 32 °C. For virus isolation, amoebae were re-suspended in 10 mL of PYG supplemented with an antibiotic mix containing 0.004 mg/mL ciprofloxacin (Cellofarm, Brazil), 0.004 mg/mL vancomycin (Sigma-Aldrich, U.S.A), and 0.020 mg/mL doxycycline (Sigma-Aldrich, U.S.A). Then, the suspension was diluted 1:10 in PBS, and inoculated in 96-well plates containing 4×10^4 cells per well. The plates were incubated for 7

days at 32 °C, and observations of the cytopathic effects were done daily using an inverted optical microscope (Quimis, Brazil). The well contents were then collected, frozen, and thawed three times to help release the viruses from intact amoeba cells. The samples were re-inoculated for two new sub-cultures on fresh amoebae, as described above (blind passages). The contents of wells with cytopathic effects were collected and inoculated into new 25 cm^2 Nunc™ Cell Culture Treated Flasks with Filter Caps (Thermo Fisher Scientific, USA) cultures containing 1 million cells. The cytopathic effects were confirmed, and these cultures were centrifuged at 1200 x *g* for lysate clearance and were further analyzed for giant viruses. Negative controls with no sample-inoculated amoeba were used in all microplates. From this collection of samples, we isolated two amoeba viruses: Niemeyer virus (Mimivirus), which was able to infect *Acanthamoeba* cells, and F. mariensis, which was able to replicate in *V. vermiformis*. These new isolates were registered at the Brazilian Biological Resources Bank, SISBIO number A237F1B.

Virus production, purification and cytopathic effect analysis

For Faustovirus production and purification, twenty T175 flasks (Thermo Fisher Scientific, USA) containing 20 million *V. vermiformis* in PYG medium were inoculated with F. mariensis at a MOI of 0.01 and incubated for 5 days, at 28°C. The lysate was centrifuged at 1200 x *g*. Then, the supernatant was collected, inoculated onto a 24% sucrose (Merck, Germany) cushion, and centrifuged at 8000 x *g* for 2 hours. The pellet was re-suspended in PBS and stored in an -80°C freezer. Three aliquots of the virus stock were titrated to the 50% end-point and calculated by the Reed-Muench method (30). Half of the viral production (600 µl) was used for biological assays and the other half (600 µl) was used for genome sequencing. For plaque forming unit (PFU) analysis, four million *V. vermiformis* cells were added to 6-well plates, forming cell monolayers. Then, the monolayers were inoculated with F. mariensis diluted ten-fold, and observed for 48 h with an optical microscope with association a digital camera (Quimis, Moticam 2300, Brazil). To test whether F. mariensis would be able to infect *V. vermiformis* cysts, T25 flasks containing 4 million cysts were inoculated with F. mariensis at MOIs of 0.01, 0.1, 1, and 10 in PBS and observed for 48h. In addition, 1 ml of these cultures were collected at

0, 4, 8, 12, and 24 hpi, and submitted to PCR targeting Faustovirus DNA polymerase to check virus replication. As previously mentioned, we had no evidence that F. mariensis was able to initiate its cycle by infecting *V. vermiformis* cysts.

Tupanvirus soda lake and Orpheovirus IHUMI LCC2 were propagated and purified as described for F. mariensis, except a 46% sucrose cushion was used during ultracentrifugation. The pellets were re-suspended in PBS and stored in an -80°C freezer. Three aliquots of each virus stock were titrated to the end-point, which was calculated by the Reed-Muench method (30).

Electron microscopy

For transmission electron microscopy (TEM) assays, *V. vermiformis* cells were infected/encysted and then were prepared for microscopy. Briefly, the medium was discarded and the monolayer gently washed twice with 0.1 M phosphate buffer. Glutaraldehyde (2.5%, v/v) was added to the system, followed by incubation for 1 h at room temperature for fixation. The cells were then collected, centrifuged at 1200 x *g* for 10 min, the medium discarded, and the cells were stored at 4 °C in phosphate buffer until electron microscopy analyses.

For the scanning electron microscopy (SEM) assays, the cells or virus particles were prepared onto round glass blades covered by poly-L-lysine and fixed with 2.5% glutaraldehyde in 0.1 M cacodylate buffer for 1 h at room temperature. Samples were then washed three times with 0.1 M cacodylate buffer and post-fixed with 1.0% osmium tetroxide for 1 h at room temperature. After a second fixation, the samples were washed three times with 0.1 M cacodylate buffer and immersed in 0.1% tannic acid for 20 min. Samples were then washed in cacodylate buffer and dehydrated by serial passages in ethanol solutions with concentrations ranging from 35–100%. They were dried at the critical CO_2 point, transferred onto stubs, and metalized with a 5 nm gold layer. The analyses were completed with scanning electronic microscopy (FEG Quanta 200 FEI) at the Center of Microscopy of UFMG, Brazil.

Genome sequencing and analyses

The F. mariensis genome was sequenced using an Illumina MiSeq instrument (Illumina Inc., San Diego, CA, USA) with the paired end application. The sequence reads were assembled de novo using ABYSS software and SPADES, and the resulting contigs were ordered by the Python-based CONTIGuator.py software. The obtained draft genomes were mapped back to verify the read assembly and close gaps. Open reading frames were predicted by GeneMarkS. The tRNA genes were searched using the tRNAscan-SE and ARAGORN software. Predicted proteins of less than 50 amino acids in length were discarded. Gene annotation was performed using Blast2GO software (31). A BLASTp search against the NCBI non-redundant (nr) database was performed, with hits being considered significative if e-values were lower than 1 x 10^{-3}. A BLASTp search was also performed with the same parameters against the cluster of orthologous groups (COGs) of proteins of the nucleocytoplasmic large DNA viruses (NCVOG) (32). In addition, we searched for conserved domains in different databases using Interproscan implemented in Blast2GO software. The genome annotation and functional classification was then manually revised and curated. Synteny analysis was performed using Mauve software (33). The DNA polymerase tree was constructed using the maximum likelihood evolution method and 1000 replicates, in MEGA 7.0 software (34).

Viral cycle and amoebal encystment characterization

The analysis of the cycle of F. mariensis by TEM was performed in the context of asynchronous infection, at an MOI of 0.1. T175 flasks containing 40 million *V. vermiformis* were inoculated with F. mariensis, and analyzed 24 hpi by TEM. A total of 250 images were evaluated in order to investigate the major steps of viral cycle.

As mentioned, during F. replication we observed substantial formation and accumulation of *V. vermiformis* cysts after infection, in especial when cells were infected at high MOIs (1 and 10). Therefore, we verify whether other *V. vermiformis* -infecting viruses would be able to trigger encystment as well. T125 flasks containing 40 million amoebas were

inoculated with F. mariensis, Tupanvirus or Orpheovirus at MOI of 10, and compared to uninfected cells. After 24 hpi, trophozoites and cysts were quantified in a Neubauer chamber (Kasvi, Brazil) and remaining cells were submitted to TEM to check whether viruses would be imprisoned inside cysts. This experiment was performed three times in triplicates.

Considering that only F. mariensis were able to remain inside *V. vermiformis* cysts, a new experiment was performed, in order to quantify cysts and trophozoites at different F. mariensis MOIs: 0.01, 0.1, 1, and 10. A total of $3x10^6$ trophozoites were added to T25 flasks with 5 ml of PYG medium and inoculated at MOIs of 0.01, 0.1, 1, or 10. After adsorption, cells were washed and then incubated for 48 hours with PYG medium. Uninfected cells were used as control. Trophozoites and cysts were quantified in a Neubauer chamber (Kasvi, Brazil).

The next step was to measure F. mariensis replication in *V. vermiformis* inoculated at different MOIs. Therefore, *V. vermiformis* cells were infected with F. mariensis at MOIs of 0.01, 0.1, 1, and 10, and incubated for 1 week. At this stage, trophozoites were no longer observed, regardless the MOI, since they either were lysed (releasing viruses to supernatant) or were converted to cysts. This longer time of incubation was designed to allow the lysis or encystment of all trophozoites in the system; therefore, at the end of the experiments, we would find viruses only in the supernatant (originated from the lysis of infected trophozoites) or inside cysts. The supernatant and cysts were separated by centrifugation (1200 x *g*, 10 min), and viral genome load was quantified by qPCR targeting the DNA polymerase gene (5'AAAACGATTCCGTGCGCAAA3'and 5`ACTAACATCGGGGCGGTTTT3`). The primers were designed using a freely available primer design tool (https://www.ncbi.nlm.nih.gov/tools/primer-blast/) at the National Center for Biotechnology Information, U.S.A (NCBI).

PCR was preceded by DNA extraction using the proteinase K/phenol-chloroform method and used at the concentration of 50 µg/µg as a template for PCR assays. PCR assays were performed using 1 µL of extracted DNA (~50 ng) in an amplification reaction mix

containing 5 µL of SYBR® Green Master Mix and 0.4 µL (10 µM) of forward and reverse primers. The final volume of the reaction was adjusted with ultrapure water to 10 µL. The conditions of the StepOne thermal cycler reactions (Applied Biosystem, USA) were: 95°C for 10 min, followed by 40 cycles of 95°C for 15 s, and 60°C for 1 min, which was followed by a final step of 95°C for 15 s, 60°C for 1 min, and 95°C for 15 s. As negative controls, we used DNA extracted from uninoculated amoebas with purified viruses or samples, and as a positive control, we used DNA from amoebae infected with purified virus. The relative quantification was performed with the delta-Ct method, and results were presented as arbitrary units (log10). This experiment was performed three times in triplicate.

Excystment assays

A stock of uninfected *V. vermiformis* cysts was produced by treating ten T175 flasks containing amoebae with NEFF solution (19) for 3 days. These cysts were quantified and stocked at room temperature. For assays of cysts containing virus, T175 flaks containing 40 million fresh trophozoites of *V. vermiformis* were infected with F. mariensis at MOIs of 0.01, 0.1, 1, and 10. One-week pi, remaining cysts were collected and washed 10 times with PBS, which was followed by 1200 x *g* centrifugation (10 min) to remove external viral particles. Cysts were then quantified in a Neubauer chamber, and then 10^5 cysts had their excystment competence evaluated after inoculation in T25 flasks containing PYG media with 5% fetal calf serum (FCS). As an excystment control, 10^5 non-infected cysts were added to a T25 flask containing PYG media with 5% FCS. In parallel, another excystment protocol was tested: the non-nutrient agar plate. Briefly, 1 mL of fresh heat-inactivated (99°C, 2 hours) *Escherichia coli* DH5-alpha (10^9 cells/ml) was added to the surface of 1% non-nutrient agar (Merck, Germany) and spread with a sterile glass Drigalski hook. After drying at room temperature, the bacterial monolayer was inoculated in eleven equidistant spots with *V. vermiformis* cysts produced at different MOIs, for a total of 10^5 cysts per agar plate. As an excystment control, 10^5 non-infected cysts were added to a control plate. The excystment rate was calculated after 3 days, by quantifying 1000 cells, three times, in triplicate.

To investigate whether cells under excystment had viruses inside of them, fresh excysted trophozoites from MOIs of 0.01 and 0.1 (excystment at MOIs of 1 and 10 was not observed) were individually collected from agar plates with sterile tips. The cells were transferred to 200-µl micro tubes, washed 3 times with 10 µl PBS, centrifuged at 1200 x *g* for 10 min, and subcultivated onto agar non-nutrient plates containing fresh heat-inactivated (99°C, 2 h) *Escherichia coli*. Cells were observed for 5 days to determine the occurrence of any cytopathic effect or encystment. After reaching 80% confluence on the agar plate, trophozoites were transferred to T25 flasks containing PYG medium, and then the presence/replication of the virus was tested by qPCR (targeting the F. mariensis DNA polymerase gene) during five subcultivations.

To investigate whether cells under excystment had F. mariensis inside their cytoplasm, T175 flasks containing 40 million fresh trophozoites of *V. vermiformis* were infected with F. mariensis at MOIs of 0.01, 0.1, 1, and 10 (three flasks per MOI). One-week pi, remaining cysts were collected and washed 10 times with PBS followed by 1200 x *g* centrifugation (10 min) to remove external viral particles. Cysts were then prepared for TEM and SEM. In parallel, those cysts were inoculated in T175 flasks containing fresh PYG medium supplemented with 5% FCS, and after 24 h, cells were prepared for TEM. The viability of cysts produced at different MOIs was assayed with 0.4% trypan blue (Sigma, U.S.A.), in a Neubauer chamber.

For cyst resistance assays, a total of 10^6 cysts produced at MOIs of 1 and 10 were submitted to 4% hydrochloric acid heated (99°C) treatments for 6, 12, 24, 48, 60, and 72 h, followed by 3 cycles of sonication at 50 kHz (30 s each), washed three times with PBS and then quantified in a Neubauer chamber. As a control, we used cysts produced under non-infectious conditions (NEFF). Those samples were also prepared for TEM, with the aim of analyzing the presence and appearance of cyst walls.

Circumvention of encystment analyses

To evaluate whether F. mariensis or Tupanvirus were able to circumvent *V. vermiformis* encystment, T25 flasks containing 4 million trophozoites were treated with a 5 ml NEFF solution, and 2 hours later, this solution was removed. The purified viruses (F. mariensis or Tupanvirus) were inoculated at a MOI of 10, 5 ml PYG medium were added to the flasks, which were then incubated for 24h at 28°C. Virus genome replication was assayed by qPCR (targeting the DNA polymerase for both viruses) (Tupanvirus primers: 5'TCACTGGTTCGTCATGCACT3' and 5'TCGCTTTGAGAGGTTTGGCT3') and cells were analyzed by TEM and optical microscopy. Cell viability was analyzed with 0.4% trypan blue in a Neubauer chamber. Alternatively, we inoculated T25 flasks containing 4 million *V. vermiformis* trophozoites with F. mariensis or Tupanvirus at a MOI of 10; after 2 h we treated the cells with 5 ml NEFF solution, and then cells were incubated for 24 h, at 28°C.

Using qPCR, we measured the expression of two serine proteinase mRNA isotypes present in *V. vermiformis* upon infection (MOI of 10) with F. mariensis or Tupanvirus or NEFF treatment. T25 flasks containing 4 million trophozoites were inoculated, and 5 h post-infection, cells were collected and submitted to RNA extraction using the RNAeasy Mini Kit (Qiagen). The samples were treated with DNase (Invitrogen) and reverse transcribed using M-MLV Reverse Transcriptase (200 U/L; Thermo Fisher Scientific), according to the manufacturer's instructions. The resulting cDNAs were used as a template in a StepOne thermocycler (Applied Biosystems) quantitative polymerase chain reaction (qPCR) assay to target two *V. vermiformis* serine proteinase mRNA isotypes (5`GACTGGTGGACGAGCTATGG`3 and 5`TCTAGGCTCGTCAAGTCCCA`3; 5`GCTAAATCGTTCACCGTGGC`3 and 5`CAACGCGTATTCATCGGCTG`3). PCR assays were performed using 1 µL of extracted DNA (50 ng) in an amplification reaction mix containing 5 µL of SYBR® Green Master Mix and 0.4 µL (10 µM) of forward and reverse primers. The final volume of the reaction was adjusted with ultrapure water to 10 µL. The conditions of the StepOne thermal cycler reactions

(Applied Biosystem, USA) were: 95°C for 10 min, followed by 40 cycles of 95°C for 15 s and 60°C for 1 min, which was followed by a final step of 95°C for 15 s, 60°C for 1 min and 95°C for 15 s. The relative quantification was performed with the delta-Ct method, and results were presented as arbitrary units (log10). This experiment was performed three times in triplicate.

Analyses of secreted factors involved in encystment

To investigate whether *V. vermiformis* cells infected by F. mariensis secrete factors were involved with the encystment, the supernatant of a culture infected at a MOI of 10 was collected 4 days pi (T175 flask, 40 million trophozoites). The supernatant was filtered with a 0.1-µm filter (Millipore, Brazil) to remove all viral particles and subsequently diluted 2-fold for inoculation in T25 flasks containing 4 million fresh *V. vermiformis* trophozoites. Similarly, supernatants from *V. vermiformis* cells infected by F. mariensis at MOIs of 0.01, 0.1, and 1 were also prepared, collected, filtered, and inoculated (undiluted) in T125 flasks containing 40 million fresh *V. vermiformis* trophozoites. To comprehend the nature *V. vermiformis* factors related to encystment, the supernatant was treated with different concentrations of proteinase K (Gibco, U.S.A.) (10, 20, 30, 40 mg/ml, 2h incubation, room temperature) followed by bromelain from pineapple stems (Sigma, U.S.A; 45 mg/ml, 24h incubation, room temperature) and enzyme inactivation. Bovine serum albumin (BSA) was used as the protease k/bromelain activity control. Treated supernatants were then inoculated into T25 flasks containing 4 million fresh *V. vermiformis* trophozoites, and their activity was evaluated regarding cyst formation.

The concentrations of potassium, calcium, and magnesium in the supernatants of cells infected with F. mariensis, Tupanvirus, and uninfected cells (control) were also assayed. For this, 96 well plates containing 4 x 10^4 *V. vermiformis* trophozoites were inoculated, and at 10 hpi, the concentrations of potassium, calcium, and magnesium were measured with a Potassium Assay Kit AB102505 (MyBioSource, U.S.A.), a Calcium Detection Assay kit (Abcam, U.S.A.) and a Magnesium Assay Kit (Sigma, U.S.A.), respectively, following manufacturer instructions. To test the potential of Mg^{2+} as an encystment inductor in *V. vermiformis*, a total of 3 nmol of

638 Mg^{2+} ($MgCl_2$, Merck, Germany) was put in a culture of 4 x 10^4 amoeba trophozoites, and the
639 rate of cyst formation from 3–12 h was measured as well as the concentration of Mg^{2+} (using a
640 Magnesium Assay Kit, Sigma, U.S.A.). The effect of ethylenediaminetetraacetic acid (EDTA)
641 (Merck, Germany) on cyst formation during F. mariensis infection was evaluated. For this, T25
642 flasks containing 4 million trophozoites were infected with F. mariensis at a MOI of 10, and 2
643 hours post infection, 10 mM EDTA were added. Flasks were incubated for 24 hours at 28°C,
644 followed by cyst counting and virus quantification by qPCR (targeting the DNA polymerase
645 gene). Results were compared to an EDTA-free control. For evaluate the effect of EDTA on the
646 inhibition of cyst formation induced by the supernatants of pre-infected trophozoites, T25 flasks
647 containing 4 million trophozoites were infected at MOIs of 0.01, 0.1, 1, and 10. After 24 hours,
648 the supernatants were collected, filtered (0.1 μm), and then inoculated into new T25 flasks
649 containing 4 million fresh amoebae. One hour post infection, 10 mM EDTA was added, and at
650 16 hpi, cysts and trophozoites were quantified in a Neubauer chamber. Results were compared
651 to EDTA-free controls, corresponding to each MOI evaluated.
652
653 **Accession number**
654 The genome sequence of Fautovirus mariensis has been submitted to Genbank under accession
655 number MK506267.
656
657 **Acknowledgements**
658 We are grateful to our colleagues from Laboratório de Vírus of Universidade Federal de Minas
659 Gerais. In addition, we thank CNPq (Conselho Nacional de Desenvolvimento Científico e
660 Tecnológico), CAPES (Coordenação de Aperfeiçoamento de Pessoal de Nível Superior),
661 FAPEMIG (Fundação de Amparo à Pesquisa do estado de Minas Gerais), Ministério da Saúde
662 (MS-DECIT) and the Microscopy Center of UFMG. F.G.F; E.G.K and J.S.A are CNPq
663 researchers. E.G.K.; B.L.S. and J.S.A. are members of a CAPES-COFECUB project.
664
665 **References**

1. Doron S, Melamed S, Ofir G, Leavitt A, Lopatina A, Keren M, Amitai G, Sorek R. 2018. Systematic discovery of antiphage defense systems in the microbial pangenome. Science (80-) 359.
2. Ratcliff F, Harrison BD, Baulcombe DC. 1997. A similarity between viral defense and gene silencing in plants. Science (80-) 276:1558–1560.
3. Brubaker SW, Bonham KS, Zanoni I, Kagan JC. 2015. Innate Immune Pattern Recognition: A Cell Biological Perspective. Annu Rev Immunol 33:257–290.
4. Secombes CJ, Zou J. 2017. Evolution of interferons and interferon receptors. Front Immunol.
5. Borden EC, Sen GC, Uze G, Silverman RH, Ransohoff RM, Foster GR, Stark GR. 2007. Interferons at age 50: Past, current and future impact on biomedicine. Nat Rev Drug Discov.
6. Bonjardim CA, Ferreira PCP, Kroon EG. 2009. Interferons: Signaling, antiviral and viral evasion. Immunol Lett.
7. Fischer MG, Hackl T. 2016. Genome Integration and Reactivation of the Virophage Mavirus In the Marine Protozoan Cafeteria roenbergensis. Nature 540:288–291.
8. Frada M, Probert I, Allen MJ, Wilson WH, de Vargas C. 2008. The “Cheshire Cat” escape strategy of the coccolithophore Emiliania huxleyi in response to viral infection. Proc Natl Acad Sci 105:15944–15949.
9. Silva LK dos S, Boratto PVM, La Scola B, Bonjardim CA, Abrahão JS. 2016. Acanthamoeba and mimivirus interactions: The role of amoebal encystment and the expansion of the “Cheshire Cat” theory. Curr Opin Microbiol 31:9–15.
10. Boratto P, Albarnaz JD, Almeida GMDF, Botelho L, Fontes ACL, Costa AO, Santos DDA, Bonjardim CA, La Scola B, Kroon EG, Abrahão JS. 2015. Acanthamoeba polyphaga Mimivirus Prevents Amoebal Encystment-Mediating Serine Proteinase Expression and Circumvents Cell Encystment. J Virol 89:2962–2965.
11. Lambrecht E, Baré J, Sabbe K, Houf K. 2017. Impact of Acanthamoeba cysts on stress

694 resistance of Salmonella enterica serovar Typhimurium, Yersinia enterocolitica 4/O:3,
695 Listeria monocytogenes 1/2a, and Escherichia coli O:26. Appl Environ Microbiol 83.
696 12. Reteno DG, Benamar S, Khalil JB, Andreani J, Armstrong N, Klose T, Rossmann M,
697 Colson P, Raoult D, La Scola B. 2015. Faustovirus, an asfarvirus-related new lineage of
698 giant viruses infecting amoebae. J Virol 89:6585–94.
699 13. Andrade AC dos SP, Rodrigues RAL, Oliveira GP, Andrade KR, Bonjardim CA, La
700 Scola B, Kroon EG, Abrahão JS. 2017. Filling Knowledge Gaps for Mimivirus Entry,
701 Uncoating, and Morphogenesis. J Virol 91:e01335-17.
702 14. Arantes TS, Rodrigues RAL, dos Santos Silva LK, Oliveira GP, de Souza HL, Khalil
703 JYB, de Oliveira DB, Torres AA, da Silva LL, Colson P, Kroon EG, da Fonseca FG,
704 Bonjardim CA, La Scola B, Abrahão JS. 2016. The Large Marseillevirus Explores
705 Different Entry Pathways by Forming Giant Infectious Vesicles. J Virol 90:5246–5255.
706 15. Silva LKDS, Andrade ACDSP, Dornas FP, Rodrigues RAL, Arantes T, Kroon EG,
707 Bonjardim CA, Abrahaõ JS. 2018. Cedratvirus getuliensis replication cycle: An in-depth
708 morphological analysis. Sci Rep 8:1–11.
709 16. Andrade AC dos SP, Miranda Boratto PV, Rodrigues RAL, Machado TB, Azevedo B,
710 Dornas FP, de Oliveira DB, Drumond BP, Kroon EG, Abrahão JS. 2018. New isolates of
711 pandoraviruses: contribution to the study of replication cycle steps. J Virol.
712 17. Lambrecht E, Baré J, Chavatte N, Bert W, Sabbe K, Houf K. 2015. Protozoan cysts act
713 as a survival niche and protective shelter for foodborne pathogenic bacteria. Appl
714 Environ Microbiol 81:5604–5612.
715 18. Fouque E, Trouilhé MC, Thomas V, Hartemann P, Rodier MH, Hécharda Y. 2012.
716 Cellular, biochemical, and molecular changes during encystment of free-living amoebae.
717 Eukaryot Cell 11:382–387.
718 19. Neff RJ, Ray SA, Benton WF, Wilborn M. 1964. Induction of synchronous encystment
719 in Acanthamoeba spp., p. 56–83. *In* Methods in cell Physiologyvolume 1. Academic
720 Press, New York.
721 20. Seed KD. 2015. Battling Phages: How Bacteria Defend against Viral Attack. PLoS

722 Pathog.
723 21. Bautista MA, Zhang C, Whitaker RJ. 2015. Virus-induced dormancy in the archaeon
724 Sulfolobus islandicus. MBio 6.
725 22. Tan D, Svenningsen S Lo, Middelboe M. 2015. Quorum sensing determines the choice
726 of antiphage defense strategy in Vibrio anguillarum. MBio 6.
727 23. Mushegian A, Medzhitov R. 2001. Evolutionary perspective on innate immune
728 recognition. J Cell Biol.
729 24. Erez Z, Steinberger-Levy I, Shamir M, Doron S, Stokar-Avihail A, Peleg Y, Melamed S,
730 Leavitt A, Savidor A, Albeck S, Amitai G, Sorek R. 2017. Communication between
731 viruses guides lysis-lysogeny decisions. Nature 541:488–493.
732 25. Barrangou R, Fremaux C, Deveau H, Richards M, Boyaval P, Moineau S, Romero DA.,
733 Horvath P. 2007. CRISPR provides acquired resistance against viruses prokaryotes.
734 Science (80-) 315:1709–12.
735 26. Jinek M, Chylinski K, Fonfara I, Hauer M, Doudna J, Charpentier E. 2012. A
736 Programmable Dual-RNA – Guided Bacterial Immunity. Science (80-) 337:816–821.
737 27. Yoshikawa G, Blanc-mathieu R, Song C, Kayama Y, Murata K, Ogata H, Takemura M,
738 Ogata H. 2019. Medusavirus, a novel large DNA virus discovered from hot spring water.
739 J Virol 1–75.
740 28. Fouque E, Yefimova M, Trouilhe M, Quellard N, Fernandez B, Rodier M, Thomas V,
741 Humeau P, Hechard Y. 2015. Morphological Study of the Encystment and Excystment
742 of Vermamoeba vermiformis Revealed Original Traits. J Eukaryot Microbiol 327–337.
743 29. Schuster FL. 2002. Cultivation of Pathogenic and Opportunistic Free-Living Amebas.
744 Clin Microbiol Rev 15:342–354.
745 30. Reed LJ, Muench H. 1938. A simple method of estimating fifty per cent endpoints. Am
746 Jounal Hyg 27:493–497.
747 31. Götz S, García-Gómez JM, Terol J, Williams TD, Nagaraj SH, Nueda MJ, Robles M,
748 Talón M, Dopazo J, Conesa A. 2008. High-throughput functional annotation and data
749 mining with the Blast2GO suite. Nucleic Acids Res 36:3420–3435.

750 32. Yutin N, Wolf YI, Raoult D, Koonin E V. 2009. Eukaryotic large nucleo-cytoplasmic
751 DNA viruses: Clusters of orthologous genes and reconstruction of viral genome
752 evolution. Virol J 6.
753 33. Darling ACE, Mau B, Blattner FR, Perna NT. 2004. Mauve: Multiple alignment of
754 conserved genomic sequence with rearrangements. Genome Res 14:1394–1403.
755 34. Kumar S, Stecher G, Tamura K. 2016. MEGA7: Molecular Evolutionary Genetics
756 Analysis Version 7.0 for Bigger Datasets. Mol Biol Evol 33:1870–1874.
757

758 **Figure legends**

759 **Figure 1: Faustovirus mariensis isolation sites, particle images, and cytopathic effects. (A)**
760 Pampulha Lagoon map with collection sites highlighted (dots). The yellow dot represents where
761 F. mariensis were collected, in front of the Pampulha Art Museum (top-right of photo). **(B-D)** F.
762 mariensis viral particles visualized by scanning **(B and C)** and transmission electron
763 microscopies. **(E-G)** Plaque forming unit (PFU) induced by F. mariensis infection in a
764 *Vermamoeba vermiformis* monolayer. In **(F)**, a close-up of a PFU shown in **(E)**, observed 24
765 hours post infection. Forty-eight hours post infection the PFUs expand and coalesce, as shown
766 in **(G)**.
767

768 **Figure 2: Gene categories and phylogeny. (A)** F. mariensis gene set classified according gene
769 predicted categories. **(B)** DNA polymerase subunit B tree, constructed using the maximum
770 likelihood evolution method and 1000 replicates. Faustovirus mariensis (pentagon) clusters with
771 other Faustovirus strains. Tree scale represents evolutionary distance.

772 **Figure 3: Electron-lucent viral factory and cytoplasmic modifications induced by**
773 **Faustovirus mariensis. (A-C)** F. mariensis presents an electron-lucent viral factory (contoured
774 in red and in detail **(B)**) not easily distinguished from the rest of the cytoplasm and observed at
775 the perinuclear region. It is possible to visualize the abundant presence of mitochondria

surrounding the viral factory (purple highlighted **(A and C)**). VF: Viral factory. N: Nucleus. Image B was obtained by TEM and graphically highlighted by using IOS image visualization software.

Figure 4: Faustovirus mariensis morphogenesis and particles organization in honeycombs-like structures. (A) F. mariensis morphogenesis begins with crescents, open structures of approximately 50 nm, which grow as an electron-dense material of the viral factory fulfills them. Particles of almost 200 nm without genomic content are observed in late phases of morphogenesis, when the genome is incorporated and centralized within several newly formed viral particles. **(B-E)** F. mariensis progeny are organized in a honeycomb fashion inside viral factories. Small honeycombs expand as new mature viruses are formed and coalesce to others in the cytoplasm **(B)**.

Figure 5: Faustovirus mariensis particles and viral factories inside *Vermamoeba vermiformis* cysts. (A) Mature *V. vermiformis* cyst enclosing a large viral factory (highlighted with a red dashed line). In **(B)**, plasma membrane is clearly visible below the thick cyst wall. For this experiment, *V. vermiformis* cells were infected with F. mariensis at MOI of 10 and prepared for transmission electron microscopy (TEM) (24 hpi).

Figure 6: *Vermamoeba vermiformis* cysts enclosing Faustovirus mariensis in different stages of viral replication cycle (A-F). The observation of more than one hundred cysts revealed the presence of F. mariensis under distinct phases of the replication cycle, including the early viral factory formation **(A-B)**, late morphogenesis/ honeycomb formation/coalescence **(C-E)** and cytoplasm fulfilled by mature viral particles **(F)**.

Figure 7: Cyst formation and viral replication at different multiplicities of infection (MOI). (A) Cyst and trophozoite quantification 48 hours after the inoculation of F. mariensis at MOIs of 0.01, 0.1, 1, and 10. The dashed line represents the input of amoebae in the beginning of the experiment (3×10^6). Uninfected cells had a natural encystment rate of 21.1%. **(B)** F.

mariensis genome quantification in the supernatants and cysts of *V. vermiformis* inoculated at different MOIs, 1 week post inoculation. The supernatants and cysts were separated by centrifugation and the viral genome load was quantified by qPCR (DNA polymerase subunit B). Error bars indicate SDs. These experiments were performed three times in triplicate.

Figure 8: Excystment assays. Cysts were produced by the inoculation of *Vermamoeba vermiformis* trophozoites with Faustovirus mariensis at MOIs of 0.01, 0.1, 1, and 10, and then their excystment potential was evaluated. **(A)** Agar plate excystment assay demonstrating that few cysts obtained from infections at MOIs of 0.01 and 0.1 were able to become trophozoites (arrows). Excystment was not observed for cysts obtained from infections at MOIs of 1 and 10. **(B)** Viability of cysts produced from infections at different MOIs (trypan blue 0.4%). Error bars indicate SDs. **(C)** Transmission electron microscopy representative image demonstrating that only uninfected cysts are able to excyst. This image corresponds to cysts obtained from infections at a MOI of 0.01, after excystment stimulus. **(D-E)** Cysts produced after infection can present either a regular shape (D) or reduced diameters and irregular shapes **(E)**. These experiments were performed three times in triplicate.

Figure 9: Faustovirus mariensis is not able to circumvent *Vermamoeba vermiformis* encystment. (A) Scheme highlighting the experimental strategy and results of an experiment testing the ability of F. mariensis and Tupanvirus to circumvent *V. vermiformis* encystment. In I and III, the encystment solution NEFF was added prior to virus inoculation. In II and IV, the viruses were inoculated before NEFF addition. **(B)** F. mariensis and **(C)** Tupanvirus genome quantification, in supernatant and cysts, for each experimental scenario analyzed (I–IV), by qPCR. The relative quantification was performed with the delta-Ct method, and results were presented as arbitrary units (log10). **(D)** Quantification of the viability of cysts (trypan blue 0.4%) produced from infections under different scenarios (I–IV). **(E)** Relative quantification of

the expression of two serine proteinase mRNA isotypes present in *V. vermiformis* upon infection (MOI of 10) with F. mariensis, Tupanvirus, or NEFF treatment. The quantification was performed 5 hours post infection or NEFF inoculation. Error bars indicate SDs. The statistical significance was calculated using a two-tailed 2-way ANOVA test and Tukey's range test, using GraphPad Prism. ***p<0.001. These experiments were performed three times in triplicate.

Figure 10: Investigation of encystment factors secreted by *Vermamoeba vermiformis*. (A) Induction of encystment (%) in *V. vermiformis* cells caused by the virus-free supernatant from a previous F. mariensis infection of a *V. vermiformis* culture (MOI of 10). Supernatant was diluted two-fold from undiluted to 1/64. **(B)** Induction of encystment (%) of *V. vermiformis* cells caused by undiluted (pure) supernatant from a previous F. mariensis infection in *V. vermiformis* culture at different MOIs. **(C–E)** Quantification of the concentration of **(C)** K^+, **(D)** Ca^{2+} and **(E)** Mg^{2+} in the supernatants of cells infected (MOI of 10, 10 hpi) with F. mariensis, Tupanvirus, and uninfected cells (control). The statistical significance was calculated using a two-tailed 2-way ANOVA test and a Tukey's range test, using GraphPad Prism. ***p<0.001. **(F)** Evaluation of the potential of Mg^{2+} as an inductor of encystment in *V. vermiformis*. A total of 3 nmol of Mg^{2+} was added to a culture of 4 x 10^4 amoeba trophozoites, and the concentration of Mg^{2+} was measured, as well as the rate of cyst formation over time. **(G and H)** Evaluation of EDTA effect on **(G)** cyst formation and **(H)** virus genome replication during F. mariensis infection, at a MOI of 10. **(I)** Evaluation of the inhibitory activity of 10 mM EDTA on the encystment process induced by supernatants of *V. vermiformis* infected by F. mariensis at different MOIs, 24 hours post inoculation. For all graphs, error bars indicate SDs. These experiments were performed three times in triplicate. **(J)** Scheme summarizing the phenomenon described in this work. Once infected by F. mariensis, a *V. vermiformis* trophozoite can be lysed, as described for other amoebal giant viruses. However, during the first events of infection in a *V. vermiformis* population, encystment factors are released into the supernatant, which can

induce the encystment of uninfected cells or even cause the encystment of infected trophozoites. As result, we found cysts under different stages of the replication cycle with no excystment ability. The overall viral load in the supernatant is controlled by *V. vermiformis* trapping a substantial amount of viral progeny inside cysts.

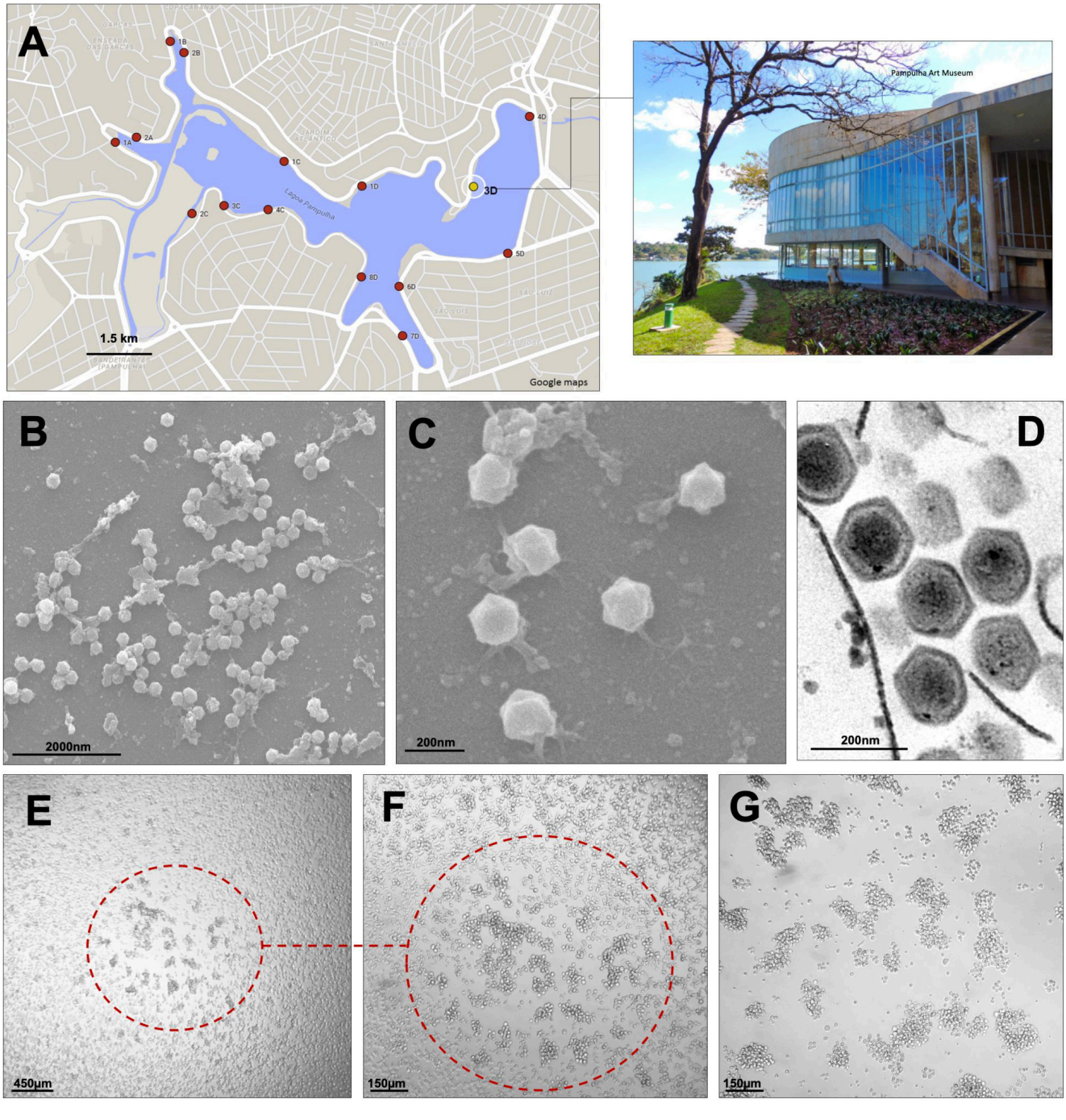

Journal of Virology

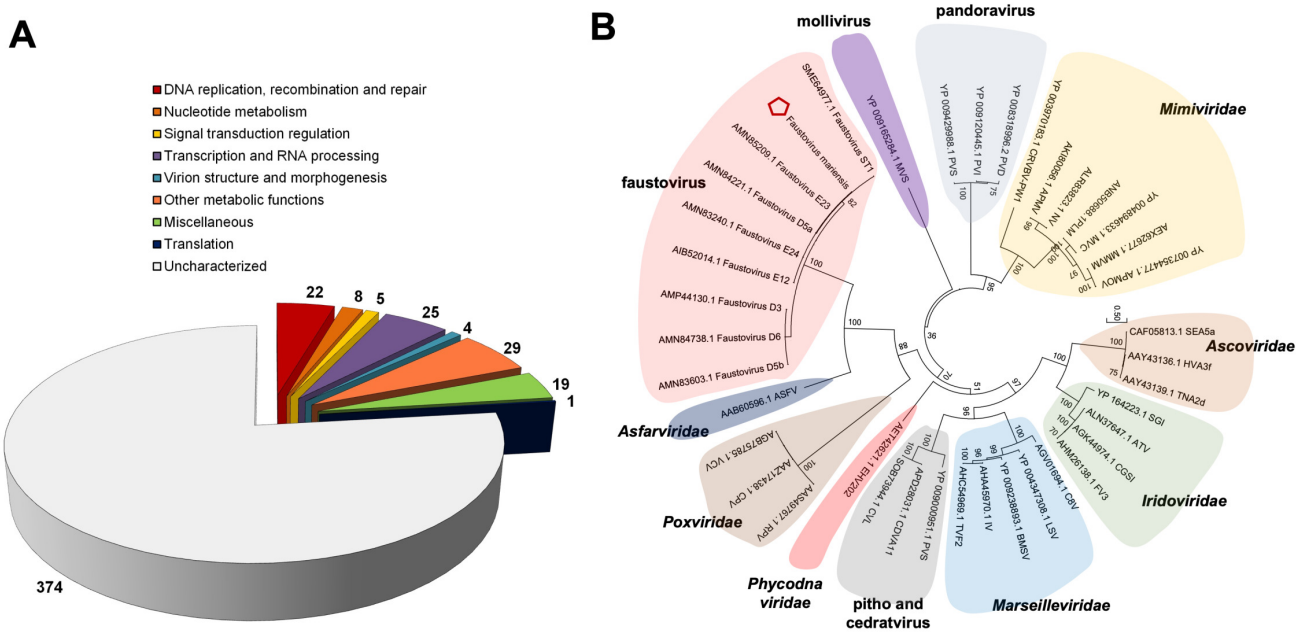

Journal of Virology
JVI
Journal of Virology